Supplementary material

Structure and properties of metal-organic frameworks precisely modulated by sulfate ions

Yuan-Yuan Guo, [a,§] Rui-Dong Wang, [a,§] Wei-Ming Wei, [a] Fang Fang, [a] Xu-Hui Zhao, [a] Suo-Shu Zhang, [a] Tian-Ze Shen [a], Jun Zhang [b], Qi-Hua Zhao*[a] and Juan Wang*[c]

[a] Key Laboratory of Medicinal Chemistry for Natural Resource, Ministry of Education and Yunnan Province, Yunnan Characteristic Plant Extraction Laboratory, School of Chemical Science and Technology, Yunnan University, 650500, People's Republic of China.

[b] New Energy Photovoltaic Industry Research Center, Qinghai University, Xining 810016, People's Republic of China.

[c] The School of Foreign Languages College, College of Arts and Sciences Kunming, Kunming, 650221, People's Republic of China.

[§] These authors contribute equally to this work.

* Corresponding author.

E-mail: qhzhao@ynu.edu.cn; 373417614@qq.com

Contents

Table S1. Crystallographic data and structure refinement parameters for MOF-**1** and MOF-**2**

Complex	**MOF-1**	**MOF-2**
chemical formula	$C_{76}H_{60.8}Cd_3N_{16}O_{8.8}S_{1.6}\cdot 1.4(H_2O_2)\cdot 6.2(H_2O)$	$C_{76}H_{60}Cd_3N_{16}O_{14}S_3\cdot 2(H_2O)\cdot 10[H_2O]$
molecular weight	1886.12	2071.13
crystal system	Monoclinic	Monoclinic
space group	*C*2	*C*2/*c*
A (Å)	31.694 (3)	32.054 (3)
b (Å)	9.6200 (8)	9.6261 (9)
c (Å)	16.0832 (13)	31.428 (3)
A (deg)	90	90
β (deg)	100.727(3)	101.060(2)
Γ (deg)	90	90
V (Å^3)	4818.0 (7)	9516.9 (14)
Z	2	4
D_x (Mg·m^{-3})	1.300	1.445
μ (MoKα) (mm^{-1})	0.75	0.82
F (000)	1788	4608
reflections	6160	8873
R_{int}	0.064	0.090
data/restraints/parameters	9050/602/566	11889/340/584
GOF on F_2	1.017	1.067
R_1/wR_2 [$I > 2\sigma(I)$]	0.0645, 0.1550	0.0735, 0.1946
R_1/wR_2 [all data]	0.1001, 0.1787	0.0963, 0.2066

[a]$R1 = \sum||F_o|-|F_c||/\sum|F_o|$, [b]$wR^2 = [\Sigma w(F_o^2 - F_c^2)^2 / \Sigma w(F_o^2)^2]^{1/2}$

Table S2. Selected bond lengths (Å) and angles (º) for MOF-**1**

Cd1—N8^{i}	2.3 (2)	C15—C25	1.418 (17)
Cd1—N8^{ii}	2.3 (2)	C16—H16	0.950
Cd1—N5^{iii}	2.249 (11)	C16—C21	1.36 (2)
Cd1—N5	2.249 (11)	C16—C22	1.390 (19)
Cd1—O13^{iv}	2.343 (13)	C17—C35	1.340 (18)
Cd1—O13^{v}	2.343 (13)	C17—N9	1.385 (16)
Cd1—N10^{i}	2.29 (10)	C18—H18	0.950
Cd1—N10^{ii}	2.29 (10)	C18—C23	1.345 (18)
Cd2—N3^{vi}	2.244 (10)	C19—H19	0.950
Cd2—N1	2.238 (14)	C20—H20	0.950
Cd2—O5	2.239 (12)	C22—H22	0.950
Cd2—O8^{vii}	2.631 (19)	C23—H23	0.950
Cd2—O14	2.304 (16)	C23—C27	1.365 (19)
Cd2—O1	2.434 (13)	C24—H24	0.950
Cd2—O2	2.986 (19)	C24—C35	1.406 (19)
N4—C6	1.428 (16)	C25—H25	0.950
N4—C19	1.412 (18)	C26—H26	0.950
N4—C29	1.369 (17)	C27—C37	1.37 (2)
N2—C21	1.452 (17)	C28—H28	0.950
N2—C30	1.350 (17)	C29—H29	0.950
N2—C32	1.352 (19)	C30—H30	0.950
N3—C9	1.392 (19)	C30—C31	1.36 (2)
N3—C29	1.294 (17)	C31—H31	0.950
N6—C27	1.439 (17)	C32—H32	0.950
N6—C34	1.363 (18)	C33—H33	0.950
N6—C36	1.430 (19)	C33—C37	1.41 (2)
N1—C31	1.35 (2)	C34—H34	0.950

N1—C32	1.36 (2)	C35—H35	0.950
C1—C8	1.493 (18)	C36—H36	0.950
C1—C24	1.40 (2)	C36—C38	1.37 (2)
C1—C25	1.376 (19)	C37—H37	0.950
C2—H2	0.950	C38—H38	0.950
C2—C7	1.414 (19)	O5—S2	1.439 (11)
C2—C28	1.342 (19)	O5—S2^{vii}	1.66 (3)
N7—C3	1.420	O5—O8^{vii}	0.48 (4)
N7—C5	1.420	O6—O7^{vii}	0.68 (4)
N7—C17	1.406 (19)	O6—S2	1.448 (11)
C3—H3	0.950	O6—S2^{vii}	1.85 (2)
C3—C4	1.420	O7—O7^{vii}	1.70 (4)
C4—H4	0.950	O7—S2	1.432 (11)
C4—N8	1.420	O7—S2^{vii}	1.14 (2)
N8—C5	1.420	S2—S2^{vii}	0.49 (2)
C5—H5	0.950	S2—O8	1.434 (11)
N5—C34	1.354 (19)	S2—O8^{vii}	1.35 (3)
N5—C38	1.398 (19)	S4—O13	1.444 (14)
C6—C20	1.34 (2)	S4—O14	1.467 (17)
C6—C28	1.394 (19)	S4—O15	1.39 (2)
C7—C12	1.472 (16)	S4—O16	1.452 (19)
C7—C14	1.401 (17)	C39—H39	0.950
C8—C10	1.496 (18)	C39—C40	1.420
C8—C12	1.356 (17)	C39—N9	1.420
C9—H9	0.950	C40—H40	0.950
C9—C19	1.358 (19)	C40—N10	1.420
C10—C18	1.397 (18)	N10—C41	1.420
C10—C33	1.35 (2)	C41—H41	0.950

C11—H11	0.950	C41—N9	1.420
C11—C21	1.381 (18)	O1—H1A	0.870
C11—C26	1.402 (18)	O1—H1B	0.870
C12—C13	1.471 (17)	O2—H2A	0.967
C13—C22	1.428 (19)	O2—H2B	0.870
C13—C26	1.377 (17)	O3—H3A^{viii}	0.869
C14—H14	0.950	O3—H3A	0.869
C14—C20	1.433 (19)	O4—H4A	0.870
C15—H15	0.950	O9—H9A	0.984
C15—C17	1.348 (19)		

Symmetry codes: (i) -*x*+1/2, *y*-1/2, -*z*; (ii) *x*-1/2, *y*-1/2, *z*; (iii) -*x*, *y*, -*z*; (iv) -*x*+1/2, *y*-1/2, -*z*+1; (v) *x*-1/2, *y*-1/2, *z*-1; (vi) *x*+1/2, *y*+1/2, *z*; (vii) -*x*+1, *y*, -*z*+1; (viii) -*x*+1, *y*, -*z*+2; (ix) *x*+1/2, *y*+1/2, *z*+1.

Table S3. Selected bond lengths (Å) and angles (º) for MOF-**2**

Cd1—O4^{i}	2.374 (9)	C34—C35	1.400 (8)
Cd1—O4^{ii}	2.374 (9)	C32—H32	0.950
Cd1—N1	2.301 (5)	C32—C30	1.383 (8)
Cd1—N1^{iii}	2.301 (5)	C37—H37	0.950
Cd1—N3^{iv}	2.285 (5)	C24—H24	0.950
Cd1—N3^{v}	2.285 (5)	C24—C25	1.384 (8)
Cd1—O5^{ii}	2.345 (9)	C3—H3	0.950
Cd1—O5^{i}	2.345 (9)	C22—H22	0.950
Cd2—O1	2.268 (9)	C22—C23	1.383 (7)
Cd2—N7	2.229 (5)	C23—H23	0.950
Cd2—N5^{iv}	2.217 (5)	C35—C33	1.392 (8)
Cd2—O6	2.29 (3)	C30—C31	1.395 (8)
Cd2—O10	2.203 (7)	C15—H15	0.950
Cd2—O7	2.282 (9)	C15—C10	1.372 (8)
S2—O6	1.455 (9)	C15—C14	1.396 (8)
S2—O14	1.449 (8)	C27—H27	0.950
S2—O11	1.447 (8)	C33—H33	0.950
S2—O3	1.447 (7)	C33—C31	1.379 (8)
S1—O1	1.479 (7)	C25—H25	0.950
S1—O4	1.467 (7)	C9—H9	0.950
S1—O8	1.458 (7)	C9—C4	1.390 (9)
S1—O12	1.465 (7)	C29—H29	0.950
N7—C37	1.328 (7)	C29—C28	1.348 (8)
N7—C38	1.364 (9)	C31—H31	0.950
N8—C37	1.348 (8)	C10—C19	1.499 (8)
N8—C35	1.438 (7)	C10—C11	1.397 (10)
N8—C36	1.365 (8)	C38—H38	0.950

N6—C26	1.430 (7)	C38—C36	1.345 (9)
N6—C27	1.353 (7)	C14—H14	0.950
N6—C29	1.372 (8)	C14—C13	1.392 (9)
N2—C3	1.333 (8)	C28—H28	0.950
N2—C4	1.430 (8)	C36—H36	0.950
N2—C2	1.363 (9)	C13—C12	1.357 (10)
N5—C27	1.304 (7)	C18—H18	0.950
N5—C28	1.392 (8)	C17—H17	0.950
N4—C13	1.425 (7)	C17—C16	1.355 (9)
N4—C18	1.348 (8)	C4—C5	1.388 (9)
N4—C16	1.386 (8)	C16—H16	0.950
N1—C3	1.310 (8)	O10—H10A	0.882
N1—C1	1.357 (10)	O10—H10B	0.882
N3—C18	1.312 (7)	C11—H11	0.950
N3—C17	1.391 (9)	C11—C12	1.401 (9)
C8—H8	0.950	C6—H6	0.950
C8—C7	1.371 (8)	C6—C5	1.389 (9)
C8—C9	1.394 (8)	C12—H12	0.950
C21—C20	1.501 (7)	C1—H1	0.950
C21—C24	1.381 (8)	C1—C2	1.359 (10)
C21—C22	1.387 (8)	C2—H2	0.950
C20—C30	1.490 (7)	C5—H5	0.950
C20—C19	1.341 (8)	O7—S1A	1.500 (9)
C26—C23	1.395 (8)	S1A—O2	1.469 (9)
C26—C25	1.386 (8)	S1A—O9	1.462 (10)
C7—C19	1.507 (7)	S1A—O5	1.476 (8)
C7—C6	1.380 (10)	O13—H13A	0.937
C34—H34	0.950	O13—H13B	0.960

C34—C32	1.375 (8)	O13—H13C	0.876

Symmetry codes: (i) -*x*+1, *y*, -*z*+1/2; (ii) *x*, -*y*+1, *z*+1/2; (iii) -*x*+1, -*y*+1, -*z*+1; (iv) *x*-1/2, *y*+1/2, *z*; (v) -*x*+3/2, -*y*+1/2, -*z*+1; (vi) *x*+1/2, *y*-1/2, *z*.

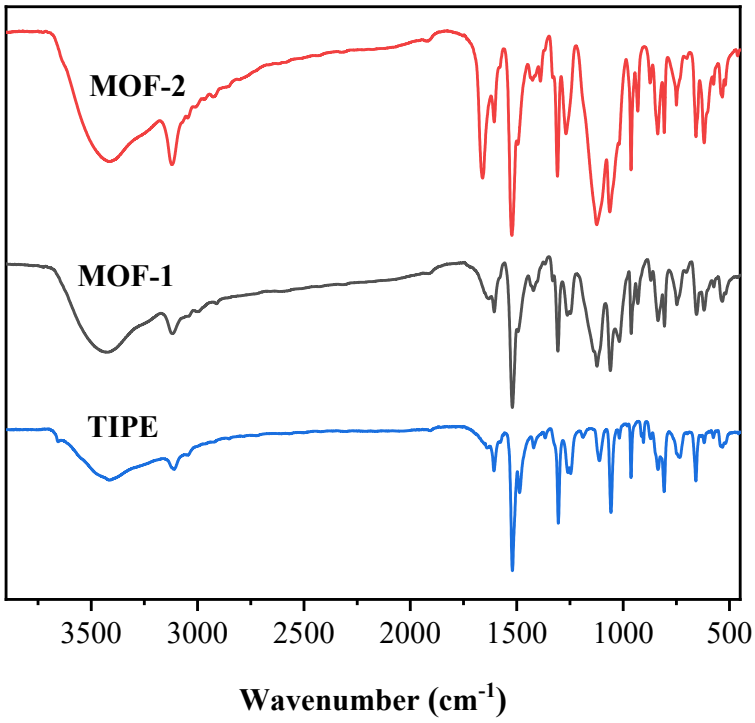

Figure S1. FT-IR of TIPE, MOF-**1** and MOF-**2**.

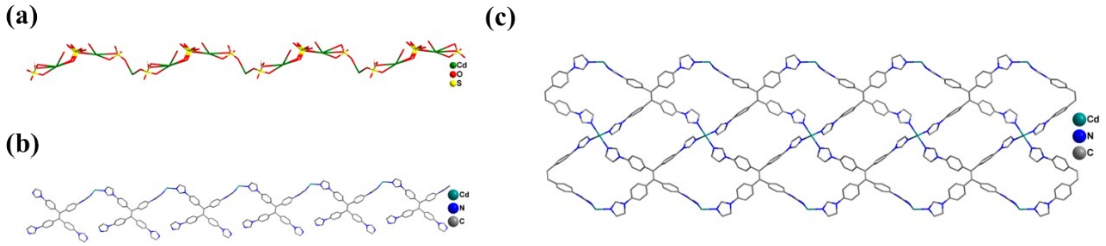

Figure S2. Coordination environment of MOF-**1** (a) One-dimensional chain composed of SO_4^{2-} and Cd; (b) One-dimensional chain composed of Cd2 and TIPE; (c) Two-dimensional layer composed of Cd1 and TIPE.

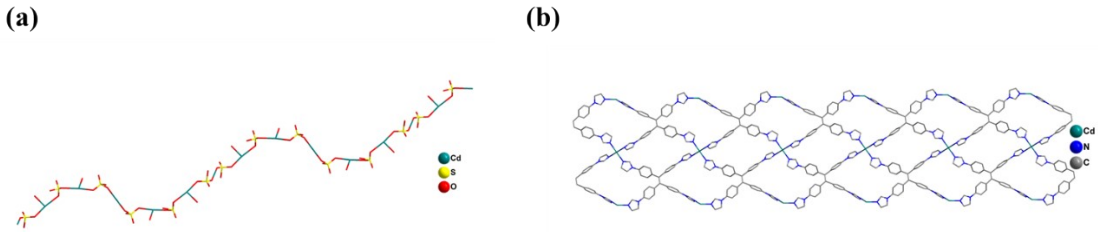

Figure S3. Coordination environment of MOF-**2** (a) One-dimensional chain composed of SO_4^{2-} and Cd; (b) Two-dimensional layer composed of Cd and TIPE.

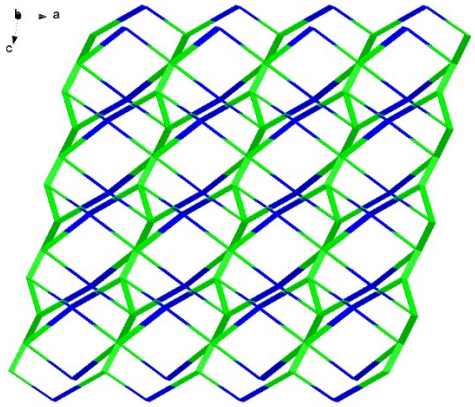

Figure S4. Schematic view of the 3D 4,4,6-connected network topology. The green nodes represent Cd(II) ions,and the blue nodes represent TIPE.

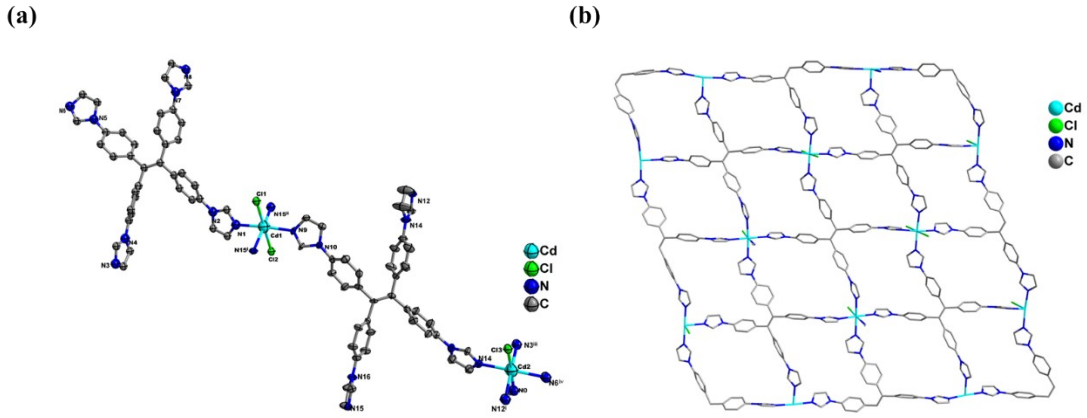

Figure S5. (a) Coordination environment of Cd(II) ions in MOF-**3**; (b) 2D structure of MOF-**3**. Symmetry codes: (i) *x*+1/2, *y*-1/2, *z*; (ii) *x*-1/2, *y*+1/2, *z*; (iii) *x*+1, *y*-2, *z*+1; (iv) *x*+1/2, *y*-3/2, *z*+1.

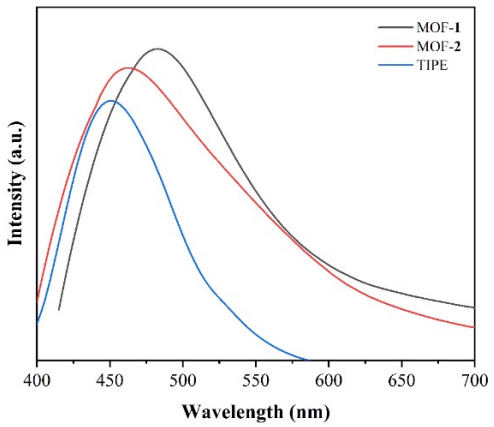

Figure S6. Solid-state fluorescence of MOF-**1** (λ_{ex} = 395 nm), MOF-**2** (λ_{ex} = 370 nm) and TIPE (λ_{ex} = 360 nm) ligands at room temperature.

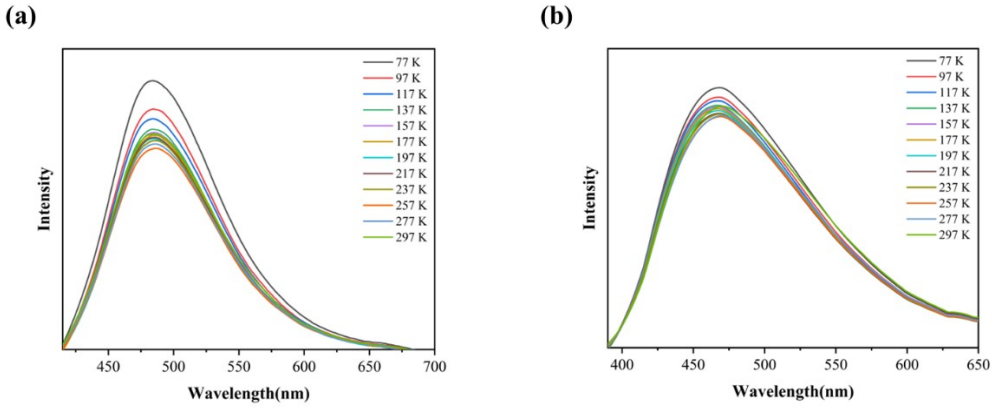

Figure S7. (a) Temperature-responsive emissions of MOF-**1** record between 77 and 297 K, (b) Temperature-responsive emissions of MOF-**2** record between 77 and 297 K.

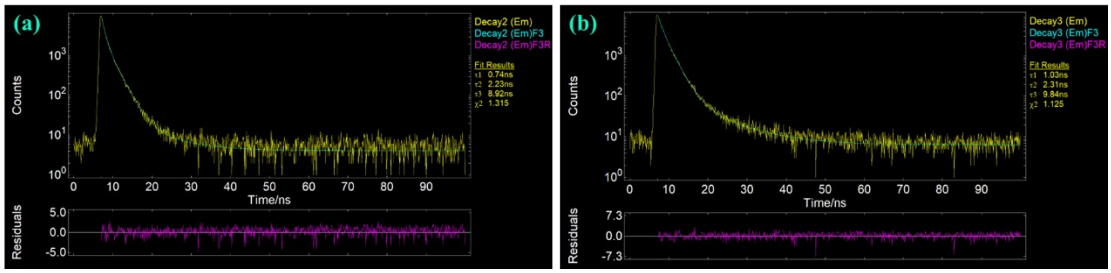

Figure S8. Luminescence decay lifetimes of MOF-**1** (a) and MOF-**2** (b) measured at the excitation (λ_{ex} = 375 nm).

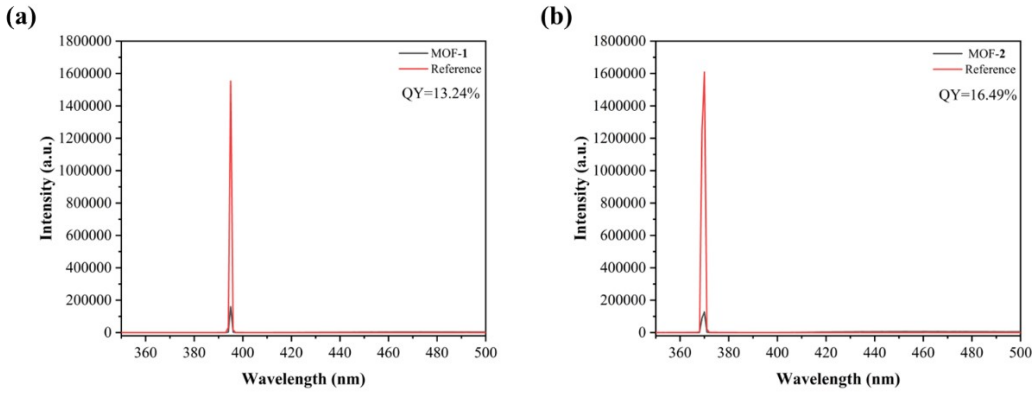

Figure S9. The fluorescence quantum yield curve measured for MOF-**1** (a) and MOF-**2** (b) powder sample at room temperature.

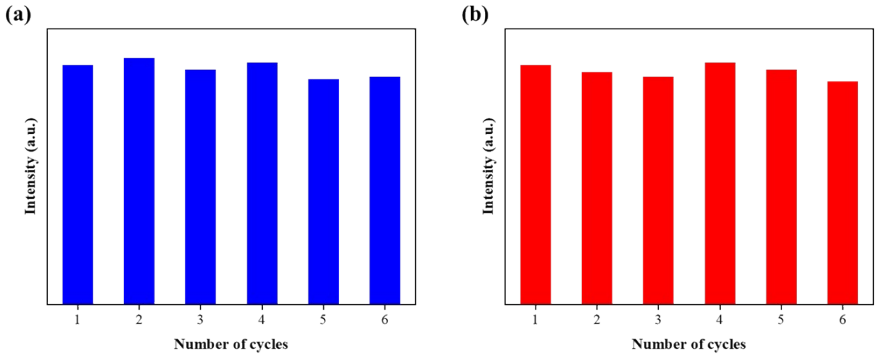

Figure S10. (a) The fluorescence intensity of Fe^{3+} ions recognized by MOF-**1** after 6 cycles; (b) the fluorescence intensity of Fe^{3+} ions recognized by MOF-**2** after 6 cycles.

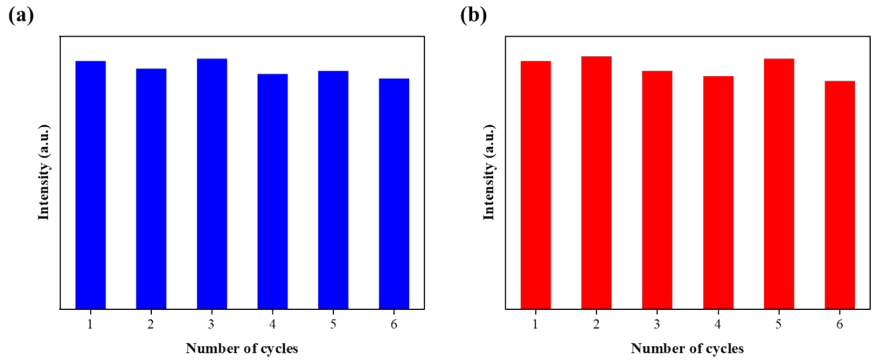

Figure S11. (a) The fluorescence intensity of $Cr_2O_7^{2-}$ ions recognized by MOF-**1** after 6 cycles; (b) the fluorescence intensity of $Cr_2O_7^{2-}$ ions recognized by MOF-**2** after 6 cycles.

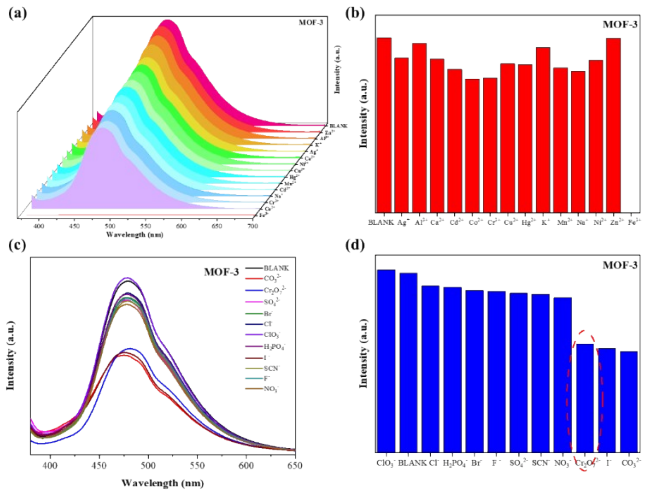

Figure S12. (a) and (b) Fluorescence spectra of MOF-**3** in the presence of different metal ions; (c) and (d) Fluorescence spectra of MOF-**3** in the presence of different anions.

MOF-**3** can recognize Fe^{3+} ions, but not $Cr_2O_7^{2-}$ ions.

Table S4. BET surface area, pore size and pore volumes of the MOFs.

Properties	MOF-**1**	MOF-**2**	MOF-**3**
BET surface area (m^2/g)	0.674	0.6622	0.2018
Langmuir surface area (m^2/g)	0.8440	1.1692	0.5801
Micropore surface area (m^2/g)	1.7895	0.7415	0.2018
Pore volume (cm^3/g)	0.002137	0.002753	0.001406
Pore size (nm)	126.81777	16.62894	29.8350

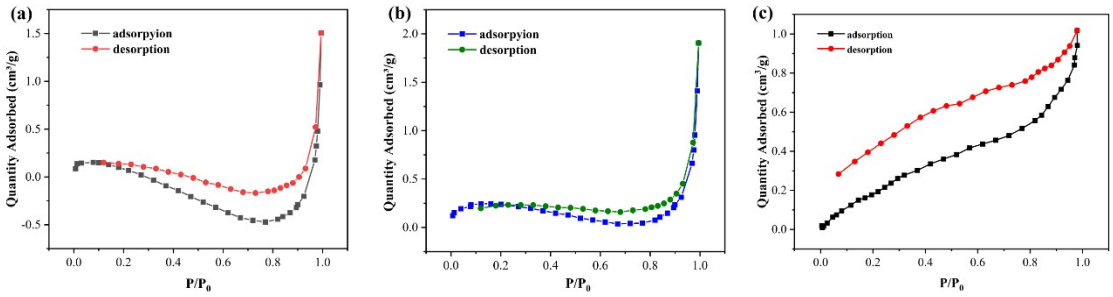

Figure S13. N_2 adsorption-desorption isotherms of MOF-**1**(a), MOF-**2**(b) and MOF-**3**(c).

From the results obtained, the pore size and the characteristic pore volumes revealed the porous nature of MOF-**1** and MOF-**2**.

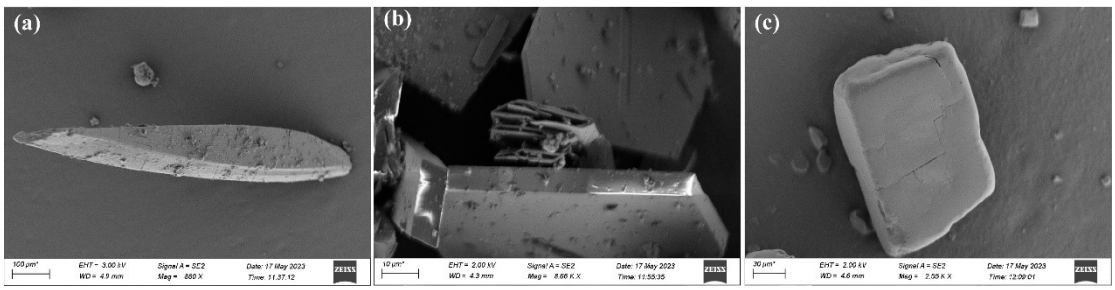

Figure S14. SEM images of MOF-**1**(a), MOF-**2**(b) and MOF-**3**(c).

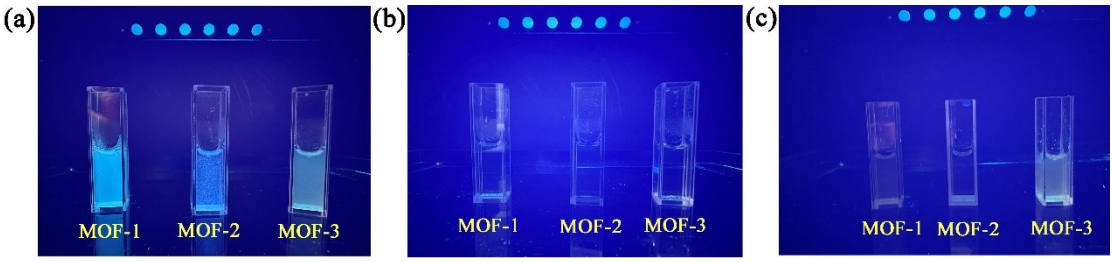

Figure S15. Fluorescence Photo of MOF-**1-3** in solvent (a), in the presence of Fe^{3+} ions (b) and $Cr_2O_7^{2-}$ ions (c).

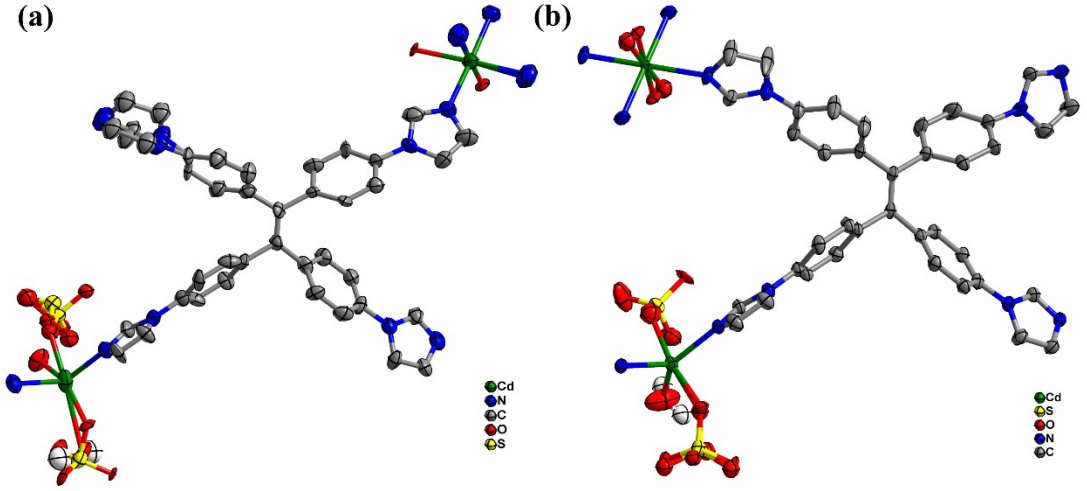

Figure S16. Ellipsoidal plots of the disordered structures of MOF-**1** and MOF-**2**.

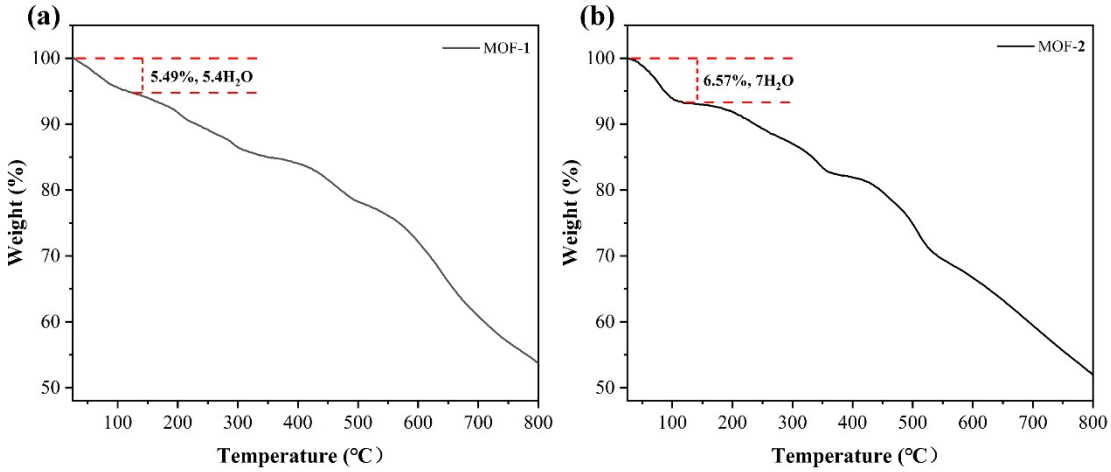

Figure S17. TGA curves of MOF-**1**(a) and MOF-**2**(b).

The TGA curves of MOF-**1** indicate that it loses 5.4 water molecules, comprising 2.4 coordinated water molecules and three free water molecules, in the temperature range of 25°C to 140°C, resulting in a weight loss of 5.49% (calculated value: 5.42%) (Figure S17a). The TGA curves of MOF-**2** show that it loses seven water molecules in the temperature range of 25°C to 112°C, leading to a weight loss of 6.57% (calculated

value: 6.26%) (Figure S17b). However, the single-crystal data results indicate the presence of nine free water molecules in MOF-**1** and ten free water molecules in MOF-**2**. This can be attributed to the natural drying process of the crystals during thermal testing, which may have caused some water to evaporate. Additionally, the presence of relatively large pores in the structure could lead to the loss of water molecules. Therefore, the number of water molecules calculated by TGA is less than that observed in the crystal data. We respect the experimental results and have written the molecular formulas based on the conclusions from the single-crystal data.

References

1. Wang, R.-D.; Zhang, W.-Q.; Zhou, S.; Tang, J.; He, M.; Zhang, S.; Du, L.; Zhao, Q.-H., A novel dual-functional coordination polymer for detection and ultra-effectively removal of Fe(III) in water. *Journal of Molecular Liquids* **2022,** *355*.

2. Wang, R. D.; He, L.; Zhu, R. R.; Jia, M.; Zhou, S.; Tang, J.; Zhang, W. Q.; Du, L.; Zhao, Q. H., Highly efficient and selective capture Pb(II) through a novel metal-organic framework containing bifunctional groups. *J. Hazard. Mater* **2022,** *427*, 127852.

3. Li, Y.; Dong, Y.; Miao, X.; Ren, Y.; Zhang, B.; Wang, P.; Yu, Y.; Li, B.; Isaacs, L.; Cao, L., Shape-Controllable and Fluorescent Supramolecular Organic Frameworks Through Aqueous Host-Guest Complexation. *Angew Chem Int Ed Engl* **2018,** *57* (3), 729-733.

4. Fan, W.; Liu, X.; Cheng, Y.; Qin, Y.; Yang, S.; Lu, Z.; Liu, Y.; Cao, Q.; Zheng, L., Two-dimensional metal-organic framework nanobelts for selective Fe^{3+} removal from aqueous solution with high adsorption capacity. *Separation and Purification Technology* **2020,** *239*.